A new linearized flow model for complex terrain

Berg, Jacob; Ott, Søren

Published in:
EWEC 2009 Proceedings online

Publication date:
2009

Document Version
Publisher's PDF, also known as Version of record

A new linearized flow model for complex terrain

Jacob Berg and Søren Ott,
Wind Energy Division, Risø National Laboratory for Sustainable Energy, DTU
jbej@risoe.dtu.dk

Abstract

We present a new linearized flow model for complex terrain. The speed of the model (seconds to minutes depending on domain size) makes it very suitable for fast estimation of wind resources and loads on wind turbines. The model is fully 3D and performs well in heterogeneously terrain including both changes in surface roughness and terrain height. The model can despite its linearity predict recirculation behind hills and is therefore superior to most linear flow models on the marked. The model is based on a linearization of the RANS equations with a turbulence closure of the eddy viscosity. A new numerical scheme solving the final system of ODEs with two-level boundary conditions has been developed. This guarantees both stability and accuracy of the obtained solutions.

Keywords: flow modeling, atmospheric boundary layer, heterogeneously terrain, ODEs and two-level boundary conditions.

1 Introduction

There is a long tradition for linear flow models in the wind energy community. The demand for fast estimation of resources and loads has made software tools such as WAsP and WEng (**www.wasp.dk**) popular with customers and clients. Both of these tools build upon a linear flow model. The strengths and weaknesses of such a choice are obvious; computational speed and a nice and simple user interface should be hold up against the lack of complex physical processes being represented in the model. Of these, one of the most challenging today is the characterization of flow around very complex terrain. CFD models, on the other hand, has the opposite attack; speed and user simplicity are critical while the modeled flow field are much more realistic and trustworthy. Since cpu speed is becoming available at a still increasing rate, the move away from linearized models towards CFD might seem obvious. We, however, find that the limit has not yet been reached, and that the linearized models can still provide very useful information about the flow even in heterogeneously terrain. We, however, needs to work out and represent the physics in a better way. The model presented in this contribution is based upon, we believe, such a way.

As we will show in this contribution, a linearized model is not necessarily the same thing as a linearized model! The traditional way goes back to Jackson and Hunt (1975) who divide the flow field up in several regions characterized by individual length scales. A length scale, l, determines the flow close to the ground where viscous effects dominates while an outer length scale, L, characterize the inviscous flow on scales comparable to the horizontal extent of the perturbation (for example a hill). These regions can then again be sub divided into two zones. The method has been very successful despite its inability to model flow separation behind steep hills.

The model proposed here originates from the two-dimensional orography model developed by Corbett et al. (2008). The starting point is the steady state RANS equations and the incompressibility equation. In this short paper we will for simplicity use the finite mixing length approximation (a $K-\epsilon$ or other higher order closure could have been used as well). The eddy diffusivity, K, is thus given by

$$K = l_m^2 \sqrt{2 S_{ij} S_{ij}}, \tag{1}$$

where $l_m = \kappa z$ and $\kappa = 0.4$. S_{ij} is the symmetric part of the velocity derivative tensor $\partial u_i / \partial x_j$.

From the equations of motion a velocity field, $u_i(\mathbf{x})$ is calculated in every grid point of the chosen domain. At present only orography and roughness can be specified and hence only velocity perturbations due to these local conditions can be modeled. The resulting velocity field $u_i(\mathbf{x})$ from a modeled scenario is thus composed of

three contributions

$$u_i(\mathbf{x}) = u_i^0(\mathbf{x}) + u_i^{1,orography}(\mathbf{x}) + u_i^{1,roughness}(\mathbf{x}). \quad (2)$$

That is, a zero order solution plus two first-order solutions due to perturbations of orography and roughness change respectively. We assume that the interaction between orography and roughness is negligible. The contribution from orography and roughness can hence be calculated individually.

2 Orography perturbations

In this section discuss the terms $u_i^0(\mathbf{x})$ and $u_i^{1,orography}(\mathbf{x})$.

First a model coordinate system, $\acute{x}_i$ is defined (to first order and hence the phrase *linearized model*):

$$x_i = \acute{x}_i + s\lambda_i(\acute{\mathbf{x}}). \quad (3)$$

Here x_i is the normal cartesian coordinate in which our domain is defined. λ is the coordinate transformation between the two coordinate systems x_i and $\acute{x}_i$. s is the expansion parameter on which the linearization and hence the model formulation will depend. We choose a model coordinate system which follows the orography closely. λ then becomes a function of the local orography height, $h(x, y)$. In

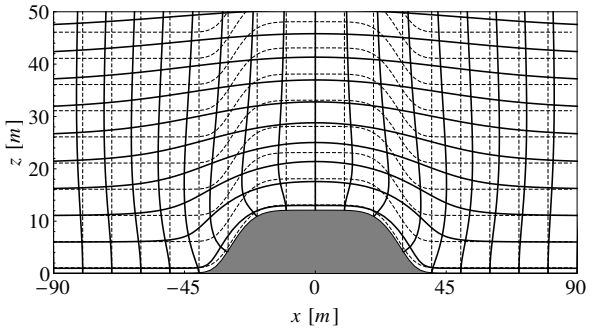

Figure 1: Terrain following coordinate systems around a simple hill. The dashed lines are the simple case in which $\lambda_3 = h(x, y)$ and $\lambda_i = 0$ for $i = 1, 2$. The solid lines are the transformation given in eqn. 4.

Figure 1 two different coordinate transformations are presented. The first (dashed lines) are the most simple in which $\lambda_3 = h(x, y)$ and $\lambda_i = 0$ for $i = 1, 2$. The second (solid lines) are given by

$$\begin{aligned} \lambda_i &= \sum_k (-\imath k_i \acute{z}) e^{-|\mathbf{k}|\acute{z}} \widehat{h}(\mathbf{k}) \mathbf{e}^{\imath \mathbf{k}\cdot\acute{\mathbf{x}}} \quad (4) \\ \lambda_3 &= \sum_k (1 + |\mathbf{k}|\acute{z}) e^{-|\mathbf{k}|\acute{z}} \widehat{h}(\mathbf{k}) \mathbf{e}^{\imath \mathbf{k}\cdot\acute{\mathbf{x}}}, \end{aligned}$$

where $i = 1, 2$ corresponds to the two horizontal directions. $\widehat{h}(\mathbf{k})$ is the Fourier transform of the local orography, $h(x, y)$.

The latter of the transformations has the obvious advantage that it follows the hill more carefully and we might therefore expect better result, as we shall later see.

We can now express the equations of motion in the new coordinate system, $\acute{x}_i$, using the simple mass conserved transformation for the velocity field, $\acute{U}_j = \frac{\partial \acute{x}_j}{\partial x_i} u_i$, where $\acute{U}_j = J\acute{u}_j$ with J being the determinant of $\frac{\partial \acute{x}_j}{\partial x_i}$. J is now a function of the expansion parameter s. We will then collect and equate terms in orders of s.

The zero order terms, $O(s^0)$, constitute flow over homogeneous terrain in the terrain following coordinate system, $\acute{x}_i$. We hence assume it to be logarithmic in the familiar way

$$\begin{aligned} \acute{u}^0 &= \cos(\theta) \frac{u_\star}{\kappa} \log(\acute{z}/\acute{z}_{00}) \quad (5) \\ \acute{v}^0 &= \sin(\theta) \frac{u_\star}{\kappa} \log(\acute{z}/\acute{z}_{00}) \quad (6) \\ \acute{w}^0 &= 0 \quad (7) \\ \acute{K}^0 &= \kappa u_\star \acute{z}. \quad (8) \end{aligned}$$

Transformed back to cartesian coordinates, the zero-order solution includes speed-up on hills and hence effects due to the local orography. Conventionally the zero-order solution in linear models does not include effects like this, but is just constant in each height.

In general the flow field, u_i, is a first order Taylor series expansion in s: $u_i = u_i^0 + s u_i^1$, where $u_i^1 = \partial u_i(s)/\partial s|_{s=0}$. For the expansion to be justified, we demand that $u_i^0 \gg s u_i^1$. Having already build in *speed-up* effects in the zero-order solution, the expansion performs much better than with conventionally linearizations.

2.1 First-order solution

Terms of order $O(s^1)$ is now studied. First we set s equal to one. We make a Fourier transformation in the two horizontal directions making all terms a function of the height, $\acute{z}$. Choosing characteristic length- and time scales as $1/k$ and $1/(ku_\star)$, where k is the length of the k-vector, $\mathbf{k}$, we can together with the non-dimensional variable, $h_k(k)$, the dimensionalize the equations. In this way all dependent variables become functions of the non-dimensional independent variables $k\acute{z}$, $k\acute{z}_0$ and the angle, α, between the wind direction, θ, and the k-vector, $\mathbf{k}$. The resulting equations are a system of non-homogeneous ODEs:

$$\frac{d}{d(k\acute{z})} \mathbf{W} = \mathbf{A}\mathbf{W} + \mathbf{S}, \quad (9)$$

where $\mathbf{W} = (\widehat{w^1}, \widehat{w^1}', \widehat{w^1}'', \widehat{w^1}''', \widehat{\Omega^1}, \widehat{\Omega^1}')$. Ω is the vertical component of vorticity while $\widehat{\ }$

indicates the the variable is Fourier transformed. The non-homogeneous term $\mathbf{S}$ includes all geometric factors arising due to the coordinate transformation.

The algebra involved in the steps described so far in this section very quickly become very tedious. We have therefore used Mathematica from Wolfram Research.

While choosing the lower boundary conditions is more or less straight forward (no-slip means that $\widehat{w^1} = \widehat{w^1}' = \widehat{\Omega^1} = 0$ at some height, $k\acute{z}_r$, dependent on $k\acute{z}_0$) (commonly known as the height of the inner surface layer) choosing the uppers is more challenging. At some height the perturbation and hence the first-order solution becomes negligible. This happens at around $k\acute{z} \sim 10$. At this height we set $\widehat{w^1} = \widehat{w^1}' = \widehat{\Omega^1} = 0$. Currently we are investigating the effect of different other upper boundary conditions. Besides changing the physics close to the top they are also quite important for numerical stability in the integration. This study is, however, not to be part of this paper.

Solving eqn. 9 together with the prescribed boundary conditions is much more difficult than it might seem at first. Specifying boundary conditions at both the surface and at some height in the atmosphere makes the final system of equations very stiff. In Corbett et al. (2008) a two-dimensional version of the model was solved with a shooting method. This method, however, failed for small values of $k\acute{z}_0$. We have tried other methods. The method of non-linear chasing has been found to work in most cases, although not always perfect. A new method which is build on the principle of *orthogonal chasing* has been developed and this method has shown to be superior to all other methods known to us. By forcing orthogonality of the boundary conditions at every height in the vertical domain we can solve a dual (a ODE involving the adjoint Hermitian of $\mathbf{A}$) problem to eqn. 9. The method is yet not published (Ott, 2008).

The final solutions, $\mathbf{W}$ to eqn. 9 are stored in handy Look-up tables (LUT). These are three-dimensional tables of the non-dimensional independent variables $k\acute{z}$, $k\acute{z}_0$ and the angle, α. These are hence independent of the local orography, $h(x, y)$, the specific wind direction, θ, the surface stress, $u_\star$, and the roughness, z_0 (here meant as the logarithmic mean surface roughness - see later on). Solving eqn. 9 will then only need to be done one time. To calculate the velocity over a given domain is hence only simple task of

1. Fourier transformation of the local orography, $h(x, y)$.
2. Interpolation from the LUT of each Fourier mode of interest.
3. Rescaling the variables in $\mathbf{W}$.
4. Inverse Fourier transformation back to physical space.
5. Transformation from terrain following coordinates, $\acute{x}_i$, to cartesian coordinates, x_i.

The last step turns out to be the most cpu demanding. Since the transformation, $\lambda_i(\acute{\mathbf{x}})$, is defined as a function of $\acute{\mathbf{x}}$, the task is non-linear. To solve it we use the optimization technique Amoeba in three dimensions (the simple coordinate transformation is only a one dimensional problem and is thus superior in speed) (Press et al., 2002).

The calculation speed of the tasks 1-5 is dependent on the specific domain size. 400×400 grid point will take no longer than one minute on a standard PC.

To illustrate the perturbation technique, we will calculate the flow around a simple symmetric hill. The hill is illustrated in Figure 2. The hill top is located in 12 m while the slope is around 40° at the steepest part. If the terrain gets too steep, a Gibbs phenomenon will occur (you can not resolve a vertical cliff by Fourier series). This can be avoided by damping all high wave numbers (frequencies). We use an exponential filter with a damping coefficient of 0.5. Another important feature of using Fourier transforms is periodic boundary conditions in the horizontal directions. Adding a large buffer zone to the domain is hence needed. How large this buffer zone should be is dependent on the size of the perturbation enforced. A rule of thumb is, however, to check whether or not the first-order solution, relaxes back to zero on the boundaries of the new enlarged domain. We might one day be able to overcome this unpleasant feature of periodic boundary conditions by using Fourier integrals combined with FFT (Press et al., 2002).

To illustrate the effect of the coordinate transformation and hence the linearization we present velocities in both coordinate transformations discussed. The results are presented in Figure 3. In the first row we see that the zero-order velocity calculated from the simple coordinate transformation is almost constant with x, while the more complex transformation has big dips around the slopes of the hill. Having these dips included in the zero-order solution for the complex transformation means, that the *job left to do* for the first-order solution is less in the case of this transformation. The linearization is thus better justified and we might hope that the final solution is closer to the true solution. Looking at

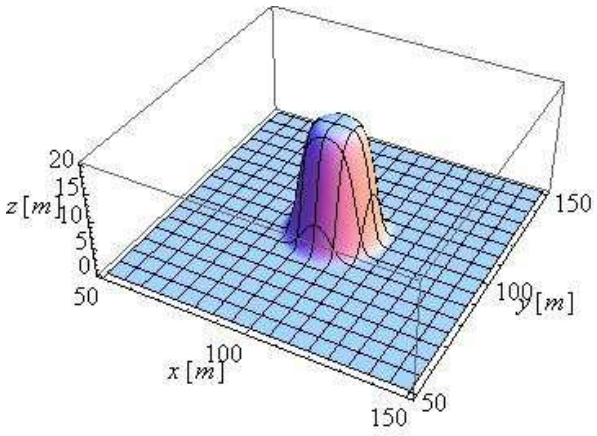

Figure 2: Simple hill used as for test purposes.

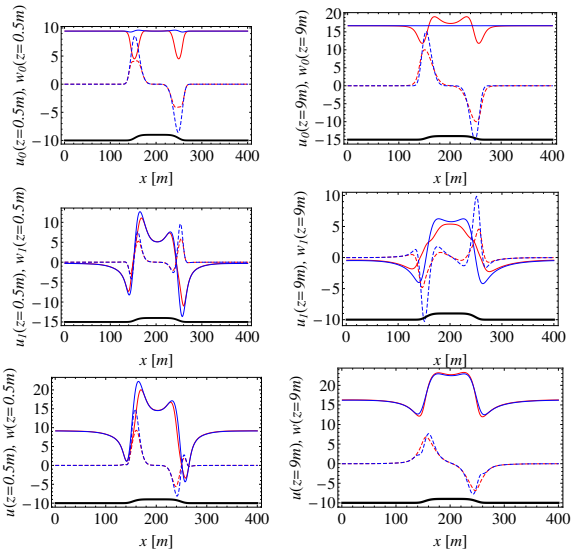

Figure 3: Velocity in fixed height over a simple hill. The *top row* is the zero-order velocity, the *middle row* is the first-order velocity while the *bottom row* is the sum of the two. The *left panels* are for 0.5 m over the terrain while the *right panels* are for 9 m. In each plot *solid curves* correspond to the horizontal velocity component along the upstream wind direction and the *dashed curves* correspond to vertical velocity. Finally *red curves* are calculated with the coordinate transformation in eqn. 4 while the *blue curves* refer to the simple transformation where $\lambda_3 = h(x, y)$ and $\lambda_i = 0$ for $i = 1, 2$. The hill is sketched in all panels.

the final solution in the bottom row, we see that both transformations predicts a small recirculation zone on the lee side of the hill close to the ground. Using the simple transformation gives for $z = 0.5$ m marginal more speed-up on the hill top and substantial higher vertical velocities. Higher up at $z = 9$ m the difference is vanishing.

We have here showed that the coordinate transformation chosen has significant impact on the results. The ones presented here are just two out of many possible transformations. They might therefore not represent the best and most ideal choices.

3 Roughness perturbations

We now turn towards roughness change and the calculation of $u_i^{1,roughness}(\mathbf{x})$. The solution to the roughness change perturbation is solved by letting the local roughness length $z_0(x, y)$ be a function of the expansion parameter s such that:

$$z_0(s) = z_{00} \left(\frac{z_0(\mathbf{x})}{z_{00}} \right)^s, \tag{10}$$

where z_{00} denote the zero order roughness length

$$z_{00} = \frac{1}{A} \int dA \log(z_0(x, y)) \tag{11}$$

that is, the roughness length in the case of a terrain with uniform roughness. $z_0(\mathbf{x})$ is the local roughness length. Due to the horizontal periodic boundary conditions a buffer zone is needed in the calculation. The size of the buffer zone, has the unfortunate effect that z_{00} changes, meaning that the size of the perturbation change. Beljaars and an P. A. Taylor (1986) used the mean logarithmic of the actually change as z_{00} instead of eqn. 11. This approach avoids the change of z_{00} with buffer size. It, however, has other problems and we will stick to the definition given by eqn. 11.

A Taylor series expansion to first order in s gives

$$z_0(s) = z_{00} + s z_{00} \log(z_0(\mathbf{x})/z_{00}). \tag{12}$$

We choose the conventional lower boundary conditions $w(z(s)) = 0$, $w'(z(s)) = 0$ and $\omega(z(s)) = 0$ which refer to a constant flux layer with no-slip. It should be emphasized that the expansion parameter, s, in this section has nothing to do with the one used in the previous section on orography.

A set of ODEs similar to eqn. 9 but this time for the first order velocity u^1 due to roughness change is then solved. In the case of orography, the non-homogeneous term S included all the information about the coordinate transformation. In the case of roughness change this term is zero and the system of ODEs becomes homogeneous. The solution method is again orthogonal chasing.

The lower boundary conditions in Fourier space can be written as:

$$\widehat{w^1} = 0 \tag{13}$$

$$\widehat{w^1}' = \imath\kappa\cos(\alpha) \tag{14}$$

$$\widehat{\Omega^1} = -\imath\kappa\sin(\alpha)$$

With these non-homogeneous boundary conditions, the problem of having orthogonal conditions at the lower boundary is fixed by Gram Smidth procedures. The height at which the lower boundary conditions are applied is set equal to the inner surface layer height, z_r. This height determines a layer of constant fluxes. It turns out that the solution is very dependent on the formulation of z_r. The different number of definitions of z_r in the literature is vast. Choosing between them is not easy. That no real qualitative experiments exist does not make the job easier.

In Figure 4 we have compared a number of different definitions of z_r with the data set presented in Bradley (1968). The roughness changes from 0.002 cm to 0.25 cm and then back again.

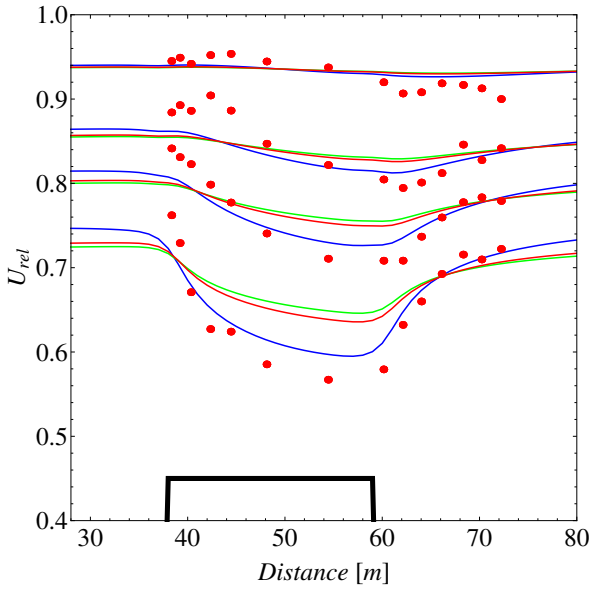

Figure 4: Horizontal velocity in four different height scaled by an upper reference speed: 0.1 m, 0.24 m, 0.45 m and 1.125 m. The reference height is 2.2 m. The dots are from the experiment by Bradley (1968). The *red curve* represents $k\acute{z}_r = kz_{00}$, the *blue curve* represents $k\acute{z}_r = \sqrt{0.3}kz_{00}^{2/3}$ and the *green curve* represent $k\acute{z}_r = \sqrt{1/8}kz_{00}^{1}.04$.

The most simple definition is $kz_r = kz_r$ (red curve). The other two definitions tested here both uses the definition by Belcher et al. (1990) in which $z_r = \sqrt{z_{00}l}$, and l being the inner length scale of the flow. This length scale can again be defined in different ways. We show two here: $kl = 0.3kz_{00}^{1/3}$ (blue curve) (Jensen et al., 1984) and $kl = 0.3kz_{00}^{0.1}$ (green curve) (Jackson and Hunt, 1975). Four different heights is studied. The blue curve is observed to fit data quite good. The agreement is, however, not striking in the upstream area (left side of the plot).

Explanations to the misfits of data and model in Figure 4 can be many. First of all the model might simply not include the right physics; the linearization does not work. Secondly the experimental setup is quite complex. Whether or not the roughness of the *smooth* surface, $z_0 = 0.002$ cm, is determined correctly is difficult to judge, the first point in the data (just at the jump) might indicate that the *smooth* roughness in the experiment was actually a factor of 10 smaller. In addition other roughness elements (sand) in the near proximity of the measurement sites could have a substantial influence on the data. Beljaars and an P. A. Taylor (1986) among others has suggested that a finite mixing length model is not suited at all to roughness changes; it overestimate the stress change. A first thing to do will therefore be to test other closures with roughness change perturbations.

4 The limit of linearized models - outlook and conclusions

In this last section we show model results for the newly instrumented and studied hill, Bolund (see Figure 5). The hill is isolated and surrounded by sea with a narrow isthmus in the east direction. The height of the hill top is 12 m and the horizontal extent is approximately 150 m $\times$ 100 m. Bolund is located just 1 km north of Risø in Denmark. The literally vertical cliff is located true west equal to the main wind direction. Even with the 2 m resolved domain utilized here it exceeds 70% making it a big challenge for most models (even CFD).

Due to the upcoming blind test for flow models (see **bolund.risoe.dk**) we can not present measured velocities for comparison with our model. Instead we have plotted the results by the fully non-linear $K - \epsilon$ CFD model Ellipsys3D developed at Risø next to ours.

Figure 5: Bolund, Denmark.

The results are presented in Figure 6 for horizontal speed-up effects ($speedup = u(x)/u(x = 0) - 1$). We have used a roughness length of $z_0 = 0.03$ m on the hill and a roughness length of $z_0 = 0.0001$ m on the sea. In order to avoid Gibbs phenomena on the cliff a rather high damping coefficient has been used $(= 2)$. Our linearized model (blue curves) predicts hill

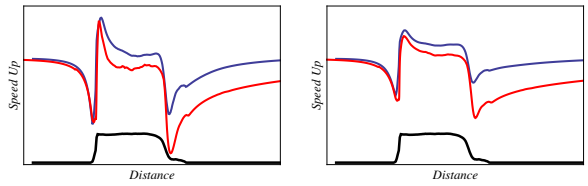

Figure 6: Results for Bolund. In the *left panel* horizontal speed-up 2 m over terrain is plotted while the *right panel* is for 5 m over terrain. The *blue curves* are velocities from our linearized model while the *red curves* are from Ellipsys3D. Due to the upcoming blind test we have omitted values on the axes.

top speed-up and hill blocking in more or less agreement with the fully non-linear Ellipsys3D. The velocities at the hill plateau are slightly larger in our model. This is mainly due to the roughness model (not shown). The lee side is the main problem. It should be noted that Ellipsys3D is *not* the truth either, it, however, performs much better in the lee side of the hill.

Predicting flow separation on the lee side, as observed in the simple case of a symmetric hill, is a strong plus for this model compared to other linearized models. The size of the zone will in most cases, however, be to small due to neglecting of non-linear effects as was observed in the Bolund case. Using a $K-\epsilon$ closure model does not give significant better results. Including second order terms $O(s^2)$ in the expansion in eqn. 3 as source terms in the system of ODEs through iteration (Xu and Taylor, 1992) might be a possible road to take in order to reach more realistic values on the lee side.

Even though one might state theat Bolund is beyond the limits set by a linearized model, the slopes encountered on Bolund is not unrealistic or far from those encountered in terrain where wind turbines are erected today. To justify the existence and usage of linearized models these extreme cases needs to be successfully modelled. Even though wind turbines are rarely put up on the lee side of a hill, the distance downstream in which the flow relaxes back to homogeneous conditions are quite often of great importance, since other wind turbines are often erected close by.

The model presented in this paper is a prominent candidate to become the next flow model of the Risø programs WAsP and WEng. The modular build of the model in which different LUT tables includes all the information about coordinate transformation, boundary conditions and turbulent closures etc. is very practical. In this way the user can have many different LUT stored on his/her PC. Comparison studies can then easily be undertaken through a simple interface program as for example WAsP and WEng which in sequence loads the different LUTs.

Of course the model is still far from operational. Central is the turbulent closure. Which kind of closure is needed. In the case of orography perturbations, a $K-\epsilon$ closure, is not that much better than the finite mixing length hypothesis employed here. Other closures will need to be investigated; a transport equation for the eddy diffusivity, K, has been developed and tested in two dimension and others will follow. In addition to the closure problem, we need more careful studies of the boundary conditions at both the bottom (the formulation of the inner surface height, z_r) and the top. For the latter including a geostrophic wind and the coriolis force seems important, since the hub height of todays wind turbines often lie well above the surface layer. Including a buoyancy term in the momentum equation and specification of heat fluxes is on the *to do* list as well.

Acknowledgments

JB would like to thank H. E. Jørgensen for taking such an interest in flow modeling for complex terrain and for allocating funding to basic research in the field. Also a great thanks to J.-F. Corbett, who left Risø quite sudden, but left me with a very well documented piece of work, which has proven to be much helpful during time spent developing this model frame work.

References

Belcher, S. E., Xu, D. P., and Hunt, J. C. R. (1990). The response of a turbulent boundary layer to arbitrary distributed two-dimensinal roughness changes. *Q. J. R. Meteorol. Soc.*, 116:611.

Beljaars, A. C. M. and an P. A. Taylor, J. L. W. (1986). A mixed spectral finite-difference model for nrutrally stratified boundary-layer flow over roughness change and topography. *Boundary-Layer Meteorol.*, 38:273.

Bradley, E. F. (1968). A micrometeorological study of vertical profiles and surface drag in the region modified by a change in surface roughness. *Q. J. R. Meteorol. Soc.*, 94:361.

Corbett, J.-F., Ott, S., and Landberg, L. (2008). A mixed spectral-integration model for neutral mean wind flow over hills. *Boundary-Layer Meteorol.*, 128:229.

Jackson, P. S. and Hunt, J. C. R. (1975). Turbulent wind flow over a low hill. *Q. J. R. Meteorol. Soc.*, 101:929.

Jensen, N. O., Petersen, E. L., and Troen, I. (1984). Extralopation of mean wind statistics with special regard to wind energy applications. *WMO-WCP 86, World Climate Programme, WMO Geneza Switherland.*

Ott, S. (2008). Solving linearized equations. *Unpublished internal Risø document*.

Press, W. H., Teukolsky, S. A., Vatterling, W. T., and Flannery, B. P. (2002). *Numerical Recipes in C++*. Cambridge University press.

Xu, D. and Taylor, P. A. (1992). A non-linear extension of the mixed spectral finite difference model for neutrally stratified turbulent flow over topography. *Boundary-Layer Meteorol.*, 59:177.